Received October 16, 2021, accepted November 4, 2021, date of publication November 15, 2021, date of current version November 24, 2021.

Digital Object Identifier 10.1109/ACCESS.2021.3128294

Fermi Velocity and Effective Mass Variations in ZGaN Ribbons: Influence of Li-Passivation

MANDAR JATKAR[1], KAMAL K. JHA[1], (Member, IEEE), AND SARAT K. PATRA[1,2], (Senior Member, IEEE)
[1]Indian Institute of Information Technology, Vadodara, Gujarat 382028, India
[2]On Lien from National Institute of Technology Rourkela, Odisha 769008, India
Corresponding author: Mandar Jatkar (201871002@iiitvadodara.ac.in)

This work was supported by the Indian Institute of Information Technology Vadodara (IIITV).

ABSTRACT The paper presents the structural stability and electronic properties of Zigzag Gallium Nitride nano ribbons(ZGaNNR) by considering the lithium(Li) atom by employing density functional theory (DFT). Li atom has been considered as a passivating element at various symmetric sites. By using Li atoms, a significant impact has been observed on the structural and electronic characteristics of ZGaNNRs. Bare@edges_both structure emerged to be the most energetically stable among other structures. For Li-passivation@edge_Ga structures, the minimum band gap has been noticed for III-V group family of nanoribbons. Interestingly, other structures of ZGaNNRs turn metallic nature irrespective of the Li site. Further, Li-bare@edge_N structure possesses the highest Fermi velocity as compared to other structures. This is useful for designing high speed interconnect applications. Further, we investigated the effective mass of various Li-ZGaNNR structures using standard two probe models. The effective mass of H-bare@edge_N structure reveals the highest effective mass in both valence and conduction bands. The proposed work proves the high capability towards the designing of the nano-scale devices.

INDEX TERMS GaNNR, passivation, Fermi velocity, effective mass.

I. INTRODUCTION

Considering the III generation era of semiconductor devices in the nano-scale regime, mainly nitrides (GaN, AIN and BN) have gained both technological and scientific attention in recent years [1], [2]. Many researchers explored the Gallium nitride nanoribbon(GaNNR) as a replacement of CMOS technology due to its wider band gap, steep reverse breakdown voltage, good thermal and chemical stability [3]–[10]. Yogi *et al.* investigated the electronic properties of Cl decorated AGaNNRs [11]. Switching phenomena and effect of NDR have been examined by Inge *et al.* using ZGaNNR by edge fluorination [12]. Ismil et al. and Xu et al. studied optical, electronic properties and also synthesized GaN [13], [14]. Sanjay *et al.* used the gallium particle trapping effect to synthesize GaN nanoparticles [15]. GaN nanoparticles are synthesized by using pulsed laser deposition, nonthermal plasma method and ammonobasic reactive sublimation [16], [17]. Thermal conductivity, phonon, analysis of charge states and noise properties have been investigated using GaNNRs [18]–[20]. Power amplifier, gunn diode, high temperature applications have been designed using GaN [21]–[23]. Mohamed Azize *et al.* designed high electron mobility transistors using GaNNR [24]. Mina Rais *et al.* used GaN as an electromechanical material [25]. Other GaN nanocomposites such as nanoribbons [26], [27], nanobelts [28], and nanotubes [29] have been synthesized. Electronic properties are studied with edge hydrogenation for graphene nanoribbons [30]. Spin states are used for ZGNR to finding outs the opto-mechanical properties [31]. Cu adsorption at different sites of AGNR structures exhibit metallic nature [32]. The qualitative characteristics of the band structures have been altered due to fluorine (F) edge functionalization [33]. The band gaps in graphene nanoribbons can be modulated with passivation techniques, and would also turn some structures metallic in nature [34]. On the other hand, exploring the effective mass and Fermi velocity of monolayer ZGaN would be useful for exploring nano-scale semiconductor devices.

The associate editor coordinating the review of this manuscript and approving it for publication was Yee Sin Ang.

II. COMPUTATIONAL DETAIL

The paper investigated the structural and electronic properties of various Li-ZGaNNRs using first-principle methods by employing DFT. ATK-VNL tool is used for calculating all

This work is licensed under a Creative Commons Attribution 4.0 License. For more information, see https://creativecommons.org/licenses/by/4.0/

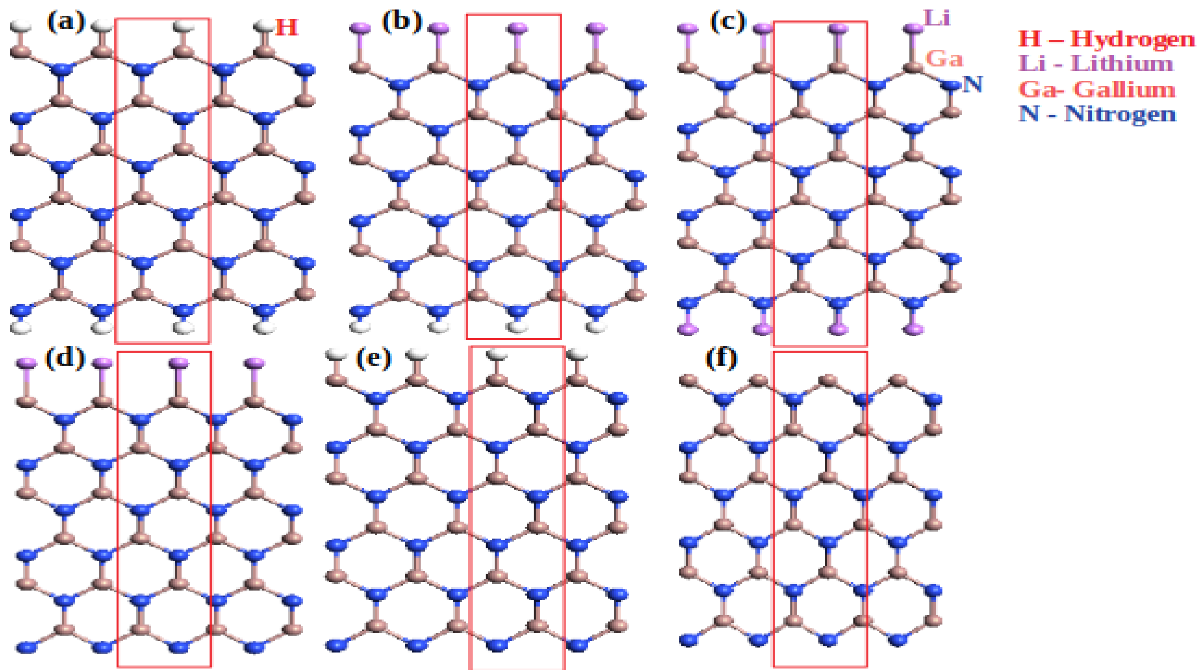

FIGURE 1. The schematic view of various Li-ZGaNNRs structures of (a) Pristine (b) Li-passivation@edge_Ga (c) Li-passivation@edges_both (d) Li-bare@edge_N (e) H-bare@edge_N and (f) Bare@edges_both structures with N_z=6.

parameters of ZGaNNRs [35]. Nanoribbons with the width N_z=6 is considered to examine the effect of Li interactions. Local-density approximations (LDA) is chosen to include the exchange-correlation [36]. For the geometrical optimization, the mess cut-off energy of 100 Ry and $1 \times 1 \times 100$ k-points sampling is used for the periodicity in the brillouin zone. The transport characteristics are investigated under the NEGF framework. The current is obtained using a two probe model using Landauer Buttiker formula [37].

III. RESULTS AND DISCUSSION

A. STRUCTURAL PROPERTIES

Various Li-passivation ZGaNNR structures are considered to analyse the thermostatic stability of GaNNRs. Figure 1(a)-(f) depict the optimized geometries of considered structures. All considered Li-passivation ZGaNNRs undergo structural changes after optimization and also noticed the change in bond length between the atoms. Table 1 summarizes the reduction or elongation of a bond length. In optimization, bond length analyses reveal that the highest edge restoration occurs at the ribbon's Ga edge with Li atom and it is increased from 1.6Å to 2.64Å for the N_z=6. To investigate structural stability, we examined the binding energy (E_{bi}) per Li atom of considered structures. Table 2 summarizes the E_{bi} calculations. E_{bi} has been analyzed using a E_{bi} = $[E_t - n_{Ga}E_{Ga} - n_N E_N - n_H E_H - n_{Li}E_{Li}]/N_t$, where E_t, E_{Ga} implies the total energy of Li-ZGaNNRs and single isolated Ga atom and E_{Li}, E_H and E_N signifies the single atom energy of Li, hydrogen and nitrogen atoms respectively. n_{Ga}, n_N, n_H, n_{Li} are the number of atoms of the respective energy. Further N_t is the total number of atoms in considered ribbon. We have varied the ZGaNNR width from 2 to 6 of various Li-ZGaNNRs to investigate binding energy and band gap. It is shown in Table 2 and Table 3. From Table 2, It is observed that width N_z=6 structures possesses

TABLE 1. The optimized bond length(before optimization) of the atoms for the Li-passivated ZGaNNRs. (All units are in Å).

Configurations	Ga-N	Ga-Li	N-Li	N-H	Ga-H
Pristine	1.81(1.61)	-	-	1.107(1.1)	1.54(1.1)
Li-passivation @edge_Ga	1.86(1.61)	2.48(1.6)	-	1.108(1.1)	-
Li-passivation @edges_both	1.87(1.61)	2.64(1.6)	1.78(1.6)	-	-
Li-bare@edge_N	1.85(1.61)	2.47(1.6)	-	-	-
H-bare@edge_N	1.81(1.61)	-	-	1.107(1.1)	1.54(1.1)
Bare@edges_both	1.84(1.61)	-	-	-	-

TABLE 2. The Calculated binding energy (E_{bi}) for the various Li-passivated ZGaNNRs.

Configurations	E_{bi}(eV)				
	2	3	4	5	6
Pristine	-5.49	-5.75	-5.99	-6.15	-6.25
Li-passivation @edge_Ga	-5.12	-5.48	-5.70	-5.91	-6.09
Li-passivation @edges_both	-4.74	-4.84	-5.19	-5.47	-5.86
Li-bare@edge_N	-4.88	-5.36	-5.63	-5.81	-5.99
H-bare@edge_N	-5.30	-5.67	-5.86	-5.99	-6.19
Bare@edges_both	-5.47	-5.60	-6.02	-5.99	-6.25

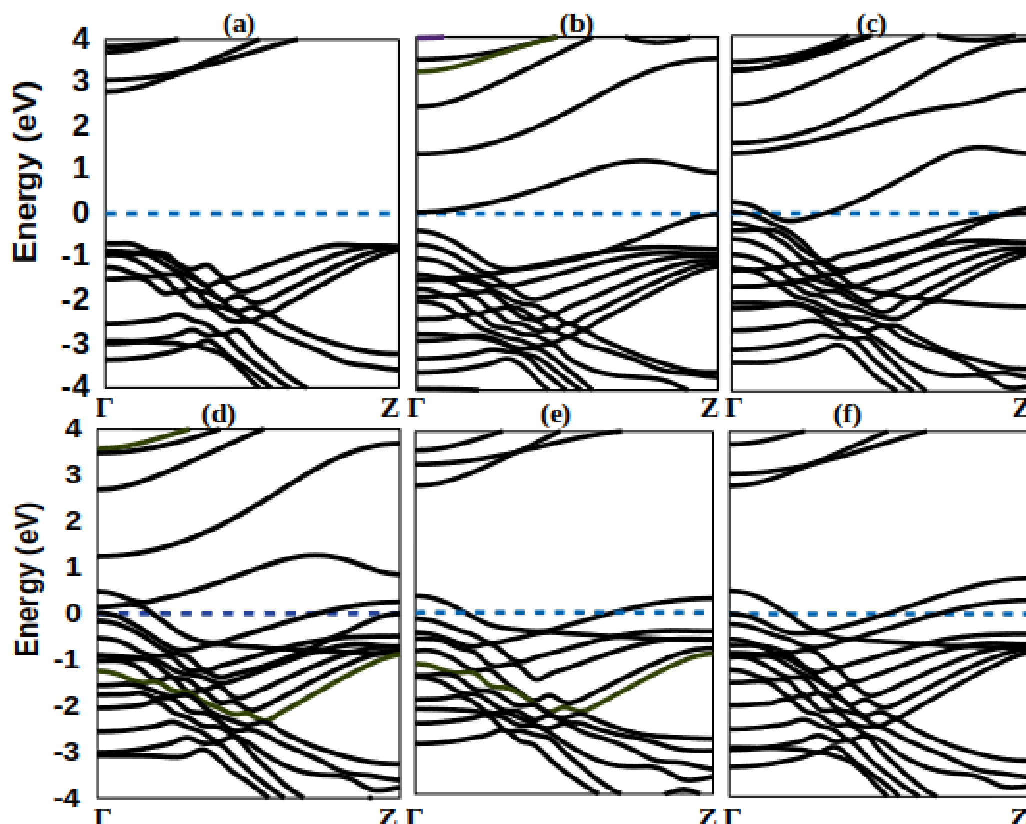

FIGURE 2. The band structures of various Li-ZGaNNR structures of (a) Pristine, (b) Li-passivation@edge_Ga, (c) Li-passivation@edges_both, (d) Li-bare@edge_N, (e) H-bare@edge_N and (f) Bare@edges_both structures with N_z=6.

TABLE 3. The Calculated band gap (E_g) for the various Li-passivated ZGaNNRs, here M implies the metallic nature of that structure.

Configurations	E_g(eV)				
	2	3	4	5	6
Pristine	2.92	4.67	2.64	2.62	3.48
Li-passivation @edge_Ga	M	M	M	M	0.043
Li-passivation @edges_both	M	M	M	M	M
Li-bare@edge_N	M	M	M	M	M
H-bare@edge_N	M	M	M	M	M
Bare@edges_both	M	M	M	M	M

a more negative value compared with width N_z=2,3,4,5. This negative value indicates that all unit cells are structurally feasible. Bare@edges_both ZGaNNR emerged to be the most thermostatically stable among other structures. The tabulated ZGaNNR binding energy (E_b) indicates the ordering of Bare@edges_both > Pristine >H-bare@edge_N >Li-passivation@edge_Ga>Li-bare@edge_N >Li-passivation@edges_both structures. The study shows that, the binding energies increase with increasing width of the ZGaNNR structures and it implies that by expanding the GaNNR width, greater stability can be achieved. Furthermore, Li-passivation@edge_Ga structure emerged as the most stable structure among other Li-ZGaNNRs.

B. ELECTRONIC PROPERTIES

The electronic properties of Li-ZGaNNRs are analyzed using E-k diagrams and DOS profiles. As seen in Figure 2(f), the metallic behavior is observed in Bare@edges_both ZGaNNR due to partially induced electronic bands and these bands are arising from dangling bonds on two side edges of the ZGaNNR. For Li-passivation@edges_both ZGaNNR, the chemical bond is formed in between Li and the edge of N/Ga atoms that saturates one dangling bond on the edge of Ga and N atom. The residual dangling bond at the Ga and N edges are present at the Fermi level as seen in Figure 2(b). In this structure, only a single electronic band passes at the Fermi level showing metallic behaviour. Among all E-k diagrams, pristine and Li-passivation@edge_Ga ZGaNNRs show the semiconductor nature. The remaining structures show metallic behavior due to dangling bonds at the edge of Ga and N atoms. The pristine ZGaNNR possesses a direct intrinsic band gap (E_g)that behaves as semiconducting in nature and a large bandgap behaviour (3.486eV) is observed in band structure. An E-k diagram and their DOS profile is calculated as shown in Figure 2(a) and 3(a). The in-direct band gap is observed 0.043eV in the case of Li-passivation@edge_Ga ZGaNNR

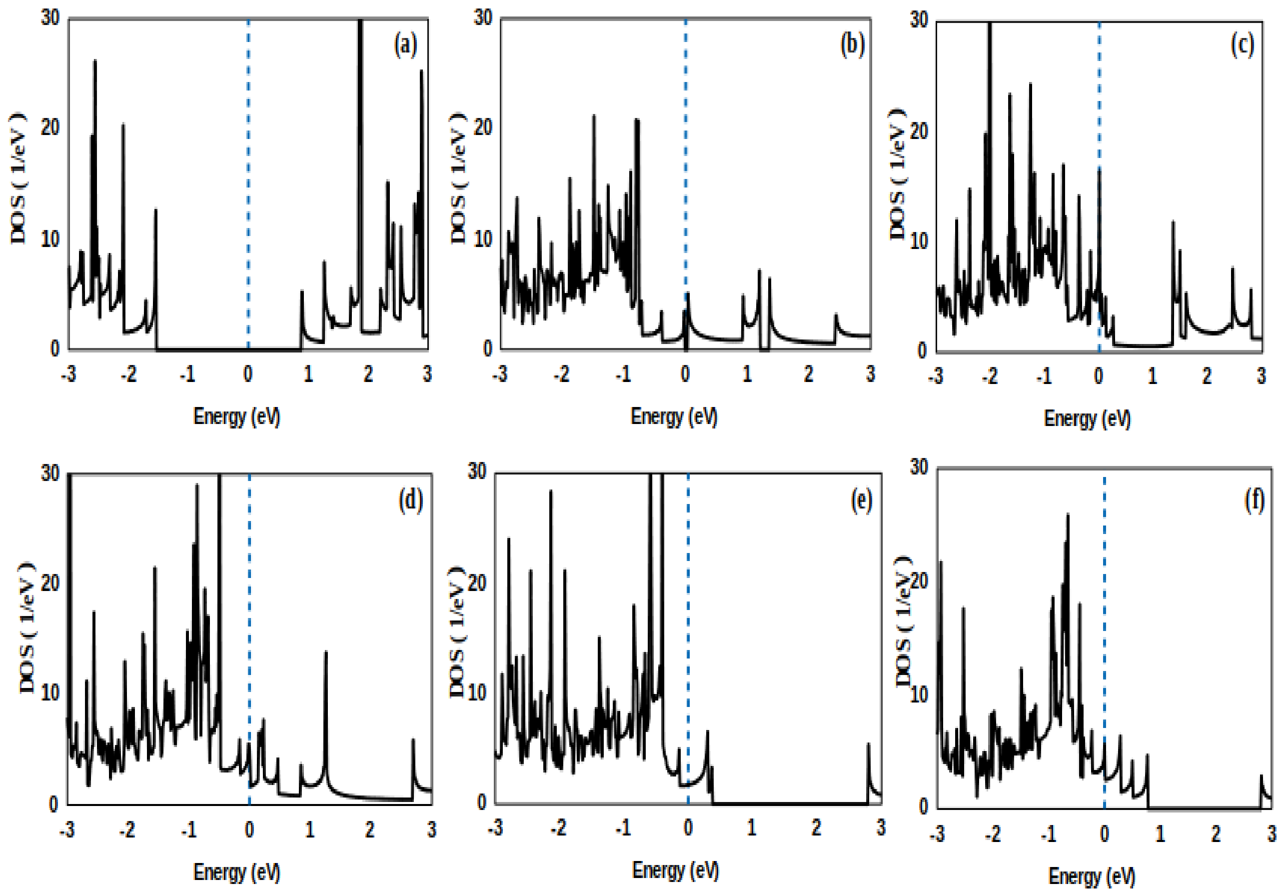

FIGURE 3. DOS profiles of various Li-ZGaNNR structures of (a) Pristine, (b) Li-passivation@edge_Ga, (c) Li-passivation@edges_both, (d) Li-bare@edge_N, (e) H-bare@ edge_N and (f) Bare@edges_both structures with N_z=6.

which clearly indicates the semi-conducting behaviour as shown Figure 2(b). This is due to π and π^* bonds of N and Ga atoms. The closing of the bandgap for Li-bare@edge_N and H-bare@edge_N structures are due to edge dangling bonds at the sites of N and Ga atoms and also noticed the presence of electronic band states around the zero Fermi level. The calculated E-k diagrams and their DOS profiles are shown in Figure 2(d-e) and Figure 3(d-e).

C. VARIATION OF FERMI VELOCITY AND EFFECTIVE MASS

A very simple way to calculate the Fermi velocity in a Dirac material is using the energy dispersion relation. The conductivity is independent of the band slope value at the Fermi level due to linear dispersion near the origin of ribbons. Another way to detect the change in the Fermi velocity is to apply Li-passivation on ZGaNNRs and also inject carriers from Li atoms to GaNNRs. With this, the conductance should increase as a function of the applied Li passivation due to the wave vector mismatch. When the position of the Li atom changes the Fermi velocity also changes. The Fermi velocity is estimated using the standard two probe models [38].

$$V_f = \frac{1}{\hbar}\frac{dE}{dk} \tag{1}$$

TABLE 4. The calculated Fermi velocity (V_f), effective mass (m^*/m_0) for the Li-passivated ZGaNNRs.

Configurations	V_f (m/s)	m^*/m_0 electron	m^*/m_0 hole
Pristine	6.87×10^4	0.223	0.123
Li-passivation @edge_Ga	7.75×10^4	0.218	0.078
Li-passivation @edges_both	7.98×10^4	0.070	0.082
Li-bare@edge_N	8.04×10^4	0.100	0.089
H-bare@edge_N	6.29×10^4	0.107	0.282
Bare@edges_both	3.92×10^4	0.135	0.221

where $\hbar$=h/2π, $\hbar$ implies the reduced Plank's constant and h is Plank's constant, value of h is 6.62 × 10^{-34} Js in SI units. The center values of energy and crystal momentum are denoted by E and k respectively. The tabulated ZGaNNR Fermi velocity (V_f) indicates the ordering of Li-bare@edge_N>Li-passivation@edges_both>Li-passivation@edge_Ga>Pristine>H-bare@edge_N>Bare @edges_both structures. It can be seen from Table 4, the

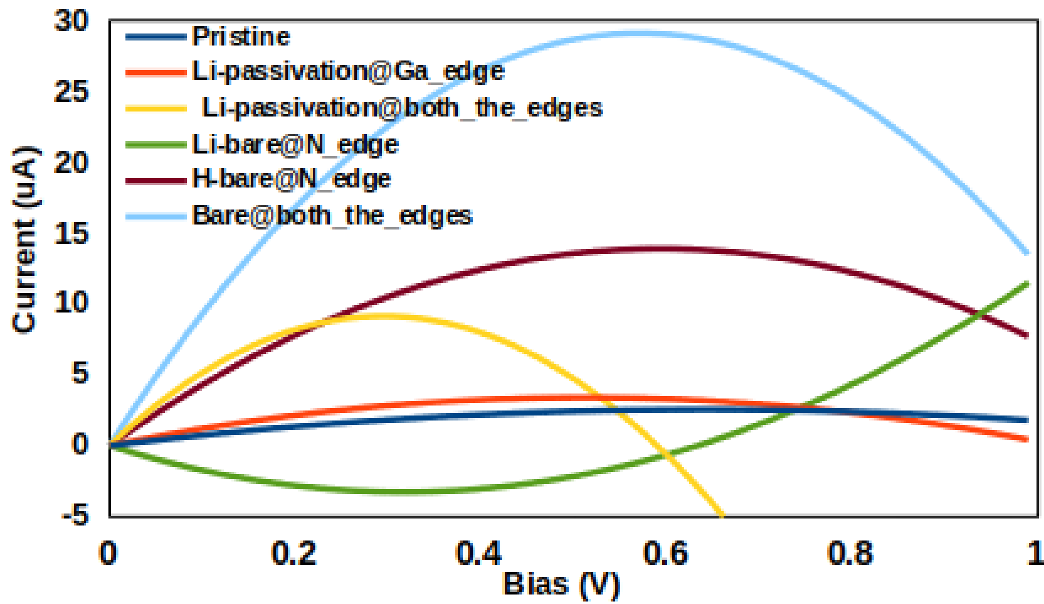

FIGURE 4. I-V characteristics of Pristine, Li-passivation@ edge_Ga, Li-passivation@edges_both, Li-bare@edge_N, H-bare@edge_N and Bare@edges_both structures of ZGaNNRs.

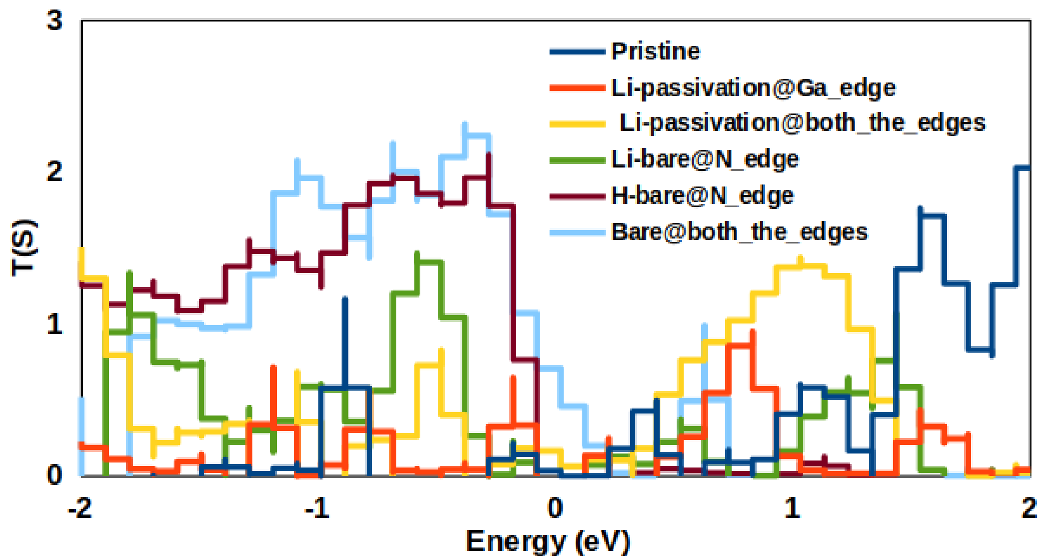

FIGURE 5. Calculated transmission spectra characteristics of Pristine, Li-passivation@edge_Ga, Li-passivation@edges_both, Li-bare@edge_N, H-bare@edge_N and Bare@edges_both structures of ZGaNNRs.

Fermi velocity(V_f) increases with increasing Li atoms in the ZGaNNR structures. Li-bare@edge_N structure possesses the highest V_f (8.04×10^4m/s) as compared with other structures. This is useful for designing high speed interconnect applications. Generally, Fermi velocity is inversely proportional to the quantum capacitance and kinetic inductance for designing high speed interconnect applications. In order to get the low inductive coupling and capacitive delay, the Fermi velocity should be high. It can be noticed from Table.4 that Li-bare@edge_N structure is the strong contender for designing nanoscale interconnect circuits. The characteristic lateral confinement of charge carriers in ZGaNNRs causes a non-zero effective charge carrier mass, which impacts on charge carrier mobility in these devices. Such a system emphasizes the importance of charge transport in order to promote future GaN based technology. Greater effective masses are observed due to the lattice Li passivation that induces quasi-particles, resulting in decreased charge mobility. In this regard, the carrier's effective mass of ZGaNNR is a main factor to design and improve GaN-based devices. Further, we investigated the effective mass (m^*/m_0) of various Li-ZGaNNR structures using standard two probe model.

The calculated effective mass (m^*/m_0) for the Li-passivated ZGaNNRs shown in Table 4. The effective mass of H-bare@edge_N structure reveals the highest effective mass in both valence (0.282) and conduction (0.107) bands. This helps to design the future low bias nano-scale semiconductor devices. The m* is calculated using a relation of energy and momentum is obtained from (2)

$$\frac{1}{m*} = \frac{1}{\hbar^2}\frac{d^2E}{dk^2} \tag{2}$$

D. TRANSPORT PROPERTIES

In this section, the transport characteristics of various Li-passivated-ZGaNNRs with $N_z = 6$ are investigated using standard two probe models. Evaluated using self-consistent methods and used bias sampling step size of 0.1V for 0 to 1V. For pristine ZGaNNR, the current-voltage curve clearly indicates that the current is rapidly enhanced during low bias, reaching a maximum value at 1.0V. The peak current around 2.5μA reaches with a voltage of 1.0V. This linearity is due to good ohmic interaction between Ga-N bonds. Further, we found Li-bare@edge_N structure is not conducting current at initial voltage up to 0.7V and afterwards its amplitude rises sharply. Li-passivation@edge_Ga structure conducts less current due to less numbers of H-atom presence in the scattering region. Li-passivation@edges_both, H-bare@edge_N and Bare@edges_both structures of ZGaNNRs exhibit NDR behaviour shown in Figure 4. The current-voltage characteristics of Bare@edges_both ZGaNNR shows that the current increased rapidly during initial positive bias, reaches at a bias of 0.6V and then decreases with an increase in voltage, showing NDR behavior. The peak current of 29.8μA was found at 0.6V and then current begins to decrease beyond 0.6V. Understanding the effect of NDR, by analyzing transmission curves, varies as a result of the voltage applied. At 0.6V, the bias window reveals a peak propagation direction with a current of approximately 29.8μA. Decreasing in current has been observed during a reduction in electron flow in the model. The NDR effect of the proposed model could be utilized in various applications. Further, we investigated the I-V characteristics of the H-bare@edge_N ZGaNNR. Current is enhanced at an initial positive bias, reached peak at 0.61V and then gradually decreases with a rise in voltage, shows a NDR effect. Further Li-passivation@edges_both ZGaNNR structure increases its current at the initial stage at 0.3V and then current decreases with a rise in voltage, indicating a NDR behavior. Figure 4 and 5 depict i-v characteristics and transmission spectra of considered Li-passivated ZGaNNRs.

IV. CONCLUSION

In this work, investigations of various Li-passivated ZGaNNRs have been carried out by employing DFT frames. The band structures and DOS of all ZGaNNRs configurations demonstrate metallic nature and can be tuned by taking Li-passivation at different edges. Li passivation ZGaNNRs reduces the electronic band gap as compared to pristine ones. Based on binding energy calculations, Bare@edges_both structure to provide found the most stable configuration as compared to other ZGaNNRs. For Li-passivation@edge_Ga structures, the minimum band gap (0.043eV) has been observed for III-V group family of nanoribbons. Further, Li-bare@edge_N structure possesses the highest Fermi velocity (8.04×10^4m/s). This makes it suitable for designing high speed interconnect applications. Further, we investigated the effective mass (m^*/m_0) of various Li-ZGaNNR structures using standard two probe models with the help of E-k relationships. The effective mass of H-bare@edge_N structure reveals the highest effective mass in both valence (0.282) and conduction (0.107) bands. This helps to design the future low bias nano-scale semiconductor devices.

ACKNOWLEDGMENT

The authors would like to thank the PDPM-Indian Institute of Information Technology Design and Manufacturing Jabalpur for providing the computational facilities and Indian Institute of Information Technology Vadodara for infrastructural facilities.

REFERENCES

[1] T. Guerra, L. Leite, S. Azevedo, and B. de Lima Bernardo, "Magnetic, electronic and optical properties of different graphene, BN and BC_2N nanoribbons," *Superlattices Microstruct.*, vol. 104, pp. 532–539, Apr. 2017.

[2] Q. Yang, R.-S. Meng, J.-K. Jiang, Q.-H. Liang, C.-J. Tan, M. Cai, X. Sun, D.-G. Yang, T.-L. Ren, and X.-P. Chen, "First-principles study of sulfur dioxide sensor based on phosphorenes," *IEEE Electron Device Lett.*, vol. 37, no. 5, pp. 660–662, May 2016.

[3] W. Saito, Y. Takada, M. Kuraguchi, K. Tsuda, I. Omura, T. Ogura, and H. Ohashi, "High breakdown voltage AlGaN-GaN power-HEMT design and high current density switching behavior," *IEEE Trans. Electron Devices*, vol. 50, no. 12, pp. 2528–2531, Dec. 2003.

[4] A. Lidow, M. De Rooij, J. Strydom, D. Reusch, and J. Glaser, *GaN Transistors for Efficient Power Conversion*. Hoboken, NJ, USA: Wiley, 2019.

[5] S. Nakamura, T. Mukai, and M. Senoh, "Candela-class high-brightness InGaN/AlGaN double-heterostructure blue-light-emitting diodes," *Appl. Phys. Lett.*, vol. 64, no. 13, pp. 1687–1689, Mar. 1994.

[6] J. Neugebauer and C. G. Van de Walle, "Hydrogen in GaN: Novel aspects of a common impurity," *Phys. Rev. Lett.*, vol. 75, no. 24, p. 4452, 1995.

[7] Z. Y. Al Balushi, K. Wang, R. K. Ghosh, R. A. Vilá, S. M. Eichfeld, J. D. Caldwell, X. Qin, Y.-C. Lin, P. A. DeSario, G. Stone, S. Subramanian, D. F. Paul, R. M. Wallace, S. Datta, J. M. Redwing, and J. A. Robinson, "Two-dimensional gallium nitride realized via graphene encapsulation," *Nature Mater.*, vol. 15, no. 11, pp. 1166–1171, Nov. 2016.

[8] H. Li, J. Dai, J. Li, S. Zhang, J. Zhou, L. Zhang, W. Chu, D. Chen, H. Zhao, J. Yang, and Z. Wu, "Electronic structures and magnetic properties of GaN sheets and nanoribbons," *J. Phys. Chem. C*, vol. 114, no. 26, pp. 11390–11394, 2010.

[9] D. Xu, H. He, R. Pandey, and S. P. Karna, "Stacking and electric field effects in atomically thin layers of GaN," *J. Phys., Condens. Matter*, vol. 25, no. 34, Aug. 2013, Art. no. 345302.

[10] M. Jatkar, K. K. Jha, and S. K. Patra, "Fe-functionalized zigzag GaN nanoribbon for nanoscale spintronic/interconnect applications," *Appl. Phys. A, Solids Surf.*, vol. 127, no. 6, pp. 1–10, Jun. 2021.

[11] R. Yogi and N. K. Jaiswal, "First-principle investigations of Cl decorated armchair GaN nanoribbons," *AIP Conf.*, vol. 2220, May 2020, Art. no. 130040.

[12] S. V. Inge, N. K. Jaiswal, and P. N. Kondekar, "Realizing negative differential resistance/switching phenomena in zigzag GaN nanoribbons by edge fluorination: A DFT investigation," *Adv. Mater. Interface*, vol. 4, no. 19, Oct. 2017, Art. no. 1700400.

[13] B. Xu and B. C. Pan, "Size-dependent electronic and optical properties of GaN nanotubes studied using LDA calculations," *Phys. Rev. B, Condens. Matter*, vol. 74, no. 24, Dec. 2006, Art. no. 245402.

[14] S. Ismail-Beigi, "Electronic excitations in single-walled GaN nanotubes from first principles: Dark excitons and unconventional diameter dependences," *Phys. Rev. B, Condens. Matter*, vol. 77, no. 3, Jan. 2008, Art. no. 035306.

[15] S. Sanjay, K. Prabakaran, and K. Baskar, "Epitaxy of gallium nitride pyramids on few layer graphene for metal-semiconductor-metal based photodetectors," *Mater. Chem. Phys.*, vol. 240, Jan. 2020, Art. no. 122189.

[16] Z. Slaiby and A. Ramizy, "Synthesis gallium nitride thin films by pulsed laser deposition as ammonia (NH_3) gas sensor," *J. Optoelectron. Biomed. Mater.*, vol. 12, no. 1, pp. 17–23, 2020.

[17] K. H. You, J. H. Kim, S. J. You, H. C. Lee, H. Ruh, and D. J. Seong, "Gallium nitride nanoparticle synthesis using nonthermal plasma with gallium vapor," *Current Appl. Phys.*, vol. 18, no. 12, pp. 1553–1557, Dec. 2018.

[18] M. A. Z. Mamun, M. Hasan, N. Mustakim, and S. Subrina, "A molecular dynamics study of thermal conductivity in monolayer GaN nanoribbon," in *Proc. IEEE Region Conf. (TENCON)*, Oct. 2019, pp. 52–56.

[19] A. J. Islam, M. S. Islam, and A. G. Bhuiyan, "Phonon properties of armchair and zigzag edged GaN nanoribbon," in *Proc. 4th Int. Conf. Electr. Inf. Commun. Technol. (EICT)*, 2019, pp. 1–6.

[20] I. Zadorozhnyi, H. Hlukhova, Y. Kutovyi, M. Petrychuk, V. Sydoruk, V. Handziuk, and S. Vitusevich, "Analysis of charge states in GaN-based nanoribbons using transport and noise studies," in *Proc. Int. Conf. Noise Fluctuations (ICNF)*, Jun. 2017, pp. 1–4.

[21] V. Camarchia, P. Colantonio, F. Giannini, R. Giofrè, T. Jiang, M. Pirola, R. Quaglia, and C. Ramella, "A design strategy for AM/PM compensation in GaN Doherty power amplifiers," *IEEE Access*, vol. 5, pp. 22244–22251, 2017.

[22] A. S. Hajo, O. Yilmazoglu, A. Dadgar, F. Kuppers, and T. Kusserow, "Reliable GaN-based THz Gunn diodes with side-contact and field-plate technologies," *IEEE Access*, vol. 8, pp. 84116–84122, 2020.

[23] A. Hassan, Y. Savaria, and M. Sawan, "GaN integration technology, an ideal candidate for high-temperature applications: A review," *IEEE Access*, vol. 6, pp. 78790–78802, 2018.

[24] M. Azize, A. L. Hsu, O. I. Saadat, M. Smith, X. Gao, S. Guo, S. Gradecak, and T. Palacios, "High-electron-mobility transistors based on InAlN/GaN nanoribbons," *IEEE Electron Device Lett.*, vol. 32, no. 12, pp. 1680–1682, Dec. 2011.

[25] M. Rais-Zadeh, V. J. Gokhale, A. Ansari, M. Faucher, D. Théron, Y. Cordier, and L. Buchaillot, "Gallium nitride as an electromechanical material," *J. Microelectromech. Syst.*, vol. 23, no. 6, pp. 1252–1271, Dec. 2014.

[26] L. Yang, X. Zhang, R. Huang, G. Zhang, and X. An, "Synthesis of single crystalline GaN nanoribbons on sapphire (0001) substrates," *Solid State Commun.*, vol. 130, no. 11, pp. 769–772, Jun. 2004.

[27] X. Xiang, C. Cao, F. Huang, R. Lv, and H. Zhu, "Synthesis and characterization of crystalline gallium nitride nanoribbon rings," *J. Cryst. Growth*, vol. 263, nos. 1–4, pp. 25–29, Mar. 2004.

[28] S. Y. Bae, H. W. Seo, J. Park, H. Yang, and S. A. Song, "Synthesis and structure of gallium nitride nanobelts," *Chem. Phys. Lett.*, vol. 365, nos. 5–6, pp. 525–529, Nov. 2002.

[29] J. Goldberger, R. He, Y. Zhang, S. Lee, H. Yan, H.-J. Choi, and P. Yang, "Single-crystal gallium nitride nanotubes," *Nature*, vol. 422, no. 6932, pp. 599–602, Apr. 2003.

[30] Y. H. Lu, R. Q. Wu, L. Shen, M. Yang, Z. D. Sha, Y. Q. Cai, P. M. He, and Y. P. Feng, "Effects of edge passivation by hydrogen on electronic structure of armchair graphene nanoribbon and band gap engineering," *Appl. Phys. Lett.*, vol. 94, no. 12, Mar. 2009, Art. no. 122111.

[31] B. M. Wong, H. Y. Simon, and G. O'Bryan, "Reversible, opto-mechanically induced spin-switching in a nanoribbon-spiropyran hybrid material," *Nanoscale*, vol. 4, no. 4, pp. 1321–1327, 2012.

[32] N. K. Jaiswal and P. Srivastava, "First principles calculations of armchair graphene nanoribbons interacting with Cu atoms," *Phys. E, Low-Dimensional Syst. Nanostruct.*, vol. 44, no. 1, pp. 75–79, Oct. 2011.

[33] K. K. Jha, N. Tyagi, N. K. Jaiswal, and P. Srivastava, "Structural and electronic properties of armchair graphene nanoribbons functionalized with fluorine," *Phys. Lett. A*, vol. 383, no. 32, Nov. 2019, Art. no. 125949.

[34] N. K. Jaiswal and P. Srivastava, "First principles calculations of cobalt doped zigzag graphene nanoribbons," *Solid State Commun.*, vol. 152, no. 15, pp. 1489–1492, Aug. 2012.

[35] M. Brandbyge, J.-L. Mozos, P. Ordejón, J. Taylor, and K. Stokbro, "Density-functional method for nonequilibrium electron transport," *Phys. Rev. B, Condens. Matter*, vol. 65, no. 16, 2002, Art. no. 165401.

[36] K. K. Jha, N. K. Jaiswal, M. Pattanaik, and P. Srivastava, "First-principle investigations for electronic transport in nitrogen-doped disconnected zigzag graphene nanoribbons," *Microelectron. Eng.*, vol. 199, Nov. 2018, pp. 96–100.

[37] H. D. Cornean, A. Jensen, and V. Moldoveanu, "A rigorous proof of the Landauer–Büttiker formula," *J. Math. Phys.*, vol. 46, no. 4, 2005, Art. no. 042106.

[38] V. Ariel and A. Natan, "Electron effective mass in graphene," in *Proc. Int. Conf. Electromagn. Adv. Appl. (ICEAA)*, Sep. 2013, pp. 696–698.

MANDAR JATKAR received the B.E. and M.Tech. degrees in electronics and communications engineering from Visvesvaraya Technological University, Karnataka, India. He is currently a full-time Ph.D. Research Scholar with the Indian Institute of Information Technology Vadodara, Gandhinagar, India. He was an Assistant Professor for over three years in Maharashtra, India. His research interests include VLSI design, nanoelectronics, and novel semiconductors.

KAMAL K. JHA (Member, IEEE) received the M.Tech. and Ph.D. degrees in VLSI design from the Indian Institute of Information Technology and Management Gwalior, India, in 2010 and 2015, respectively. He is currently an Assistant Professor at IIIT Vadodara, India. His research interests include VLSI and embedded systems, nanoelectronics, and novel semiconductors devices.

SARAT K. PATRA (Senior Member, IEEE) received the B.Sc. (Eng.) degree in electronics and telecommunication engineering from UCE Burla, in 1986, the M.Sc. (Eng.) degree in electronics system and communication specialization from NIT Rourkela, and the Ph.D. degree from The University of Edinburgh, U.K., in 1998. He is currently working as the Director of the Indian Institute of Information Technology Vadodara, Gujarat, India. He has served the Defence Research and Development Organization (DRDO), for a short period before moving to the National Institute of Technology Rourkela, in 1989. He has supervised 16 Ph.D. students and published over 60 articles in refereed journals besides more than 150 conference papers. His research interests include adaptive signal processing, fuzzy systems, wireless communication, and machine learning for wireless communication networks, and related fields. He was a recipient of the prestigious Common-Wealth Scholarship.

• • •